Check for updates

Concrete Plates Reinforced with Embedded CFRP Rods and Carbon/Steel Strips

Elisa Bettucci[1], Roberto Capozucca[1](✉), Abdelwahhab Khatir[1], Samir Khatir[2], and Erica Magagnini[1]

[1] Structure Section DICEA, Polytechnic University of Marche, Ancona, Italy
r.capozucca@staff.univpm.it
[2] Faculty of Civil Engineering, Ho Chi Minh City Open University, Ho Chi Minh City, Vietnam

Abstract. Plates and shells are structural elements present in many civil constructions. These elements are usually built with reinforced concrete or prestressed concrete for considerable plane dimensions. The use of FRP rods during casting instead steel bars may allow to improve the behaviour under high loading and durability avoiding corrosion processes of steel. This work presents an investigation about the behaviour of concrete rectangular plates without steel bars reinforcing in tension. An experimental campaign was carried out on orthotropic and isotropic rectangular concrete plates reinforced, respectively, with carbon fibre polymer (CFRP) rods and carbon/steel fibre (C/SF) strips embedded in concrete in the tensile side. Static load was applied on the centres area of plate models. Evolution of cracking and deflections were monitored during experimental tests and results are shown and discussed.

Keywords: Concrete plate · CFRP rods · Carbon/steel fibres · Bending test

1 Introduction

The use of composite material such as Fibre Reinforced Polymers (FRPs) is growing in civil engineering field especially in the structural rehabilitation of damaged RC beams or to retrofit RC elements [1, 2].

FRPs systems can be found in the form of lamina, strips, reinforcing bars and meshes. The most adopted fibres are Carbon, Glass, Basalt and Aramid; furthermore, in recent years there is an increasing interest in the use of natural fibres for FRPs systems [3].

The main techniques usually adopted in the RC concrete elements like beams and columns consist in the use of FRP lamina/strips glued on the concrete surface or FRP rods/strips inserted into grooves in the cover of sections. This last technique is characterized by near surface mounted FRPs and it represents a convenient method to limit some problems linked to the use of strengthening externally bonded FRP lamina/strips [4–6]. Experimental results confirmed availability of strengthening with FRPs [7–13]. Other investigations analysed the possibility to use fibres embedded in cement matrix [14–17]. Recently, innovative technique based on soft computing have been adopted to

© The Author(s), under exclusive license to Springer Nature Switzerland AG 2023
R. Capozucca et al. (Eds.): ICSCES 2022, LNCE 317, pp. 70–81, 2023.
https://doi.org/10.1007/978-3-031-24041-6_6

civil engineering problems [18–20]. New frontiers of research are focused on the implementation of artificial neural network (ANN) models for structural behaviour prediction of RC plates strengthened with FRP [20].

This paper describes an experimental investigation carried out to evaluate the bending behaviour of two concrete thin plates reinforced with carbon and steel fibres (C/SF) without use of polymeric matrix. In this way the concrete becomes as matrix for fibres which substitute the steel bars in the tensile zone of plate under loading. Moreover, the bending behaviour of an orthotropic plate consisting of a grid of beams and reinforced with CFRP bars is also analysed.

Two concrete thin plate specimens are reinforced, respectively, with carbon and steel fibres located as a net during the casting of concrete on a plane at 15 mm from concrete surface. The third concrete plate specimen is characterized by two orders of concrete beams in the plane principal directions. Beams are reinforced with CFRP rods, composite material represented by carbon fibres in a polymeric matrix of epoxy resin.

These plates were subjected to a same loading path until failure and experimental results are discussed below.

The behaviour of isotropic plates confirms availability of use of dry fibres as a net in the tensile concrete zone although the bond mechanisms have a great influence on the response.

2 Rectangular Plate Model and Bending Tests Setup

2.1 Isotropic Plate Models

Two concrete thin plate models have been built in laboratory with dimensions 1.0 m·1.0 m in plan and thickness 50 mm (Fig. 1. Rectangular isotropic plate models: (a) plate model with CF strips; (b) plate model with SF strips.) [21]. One of two plates has been reinforced in the tensile side with a net of orthogonal strips of Carbon Fibre (CF) (Fig. 1. Rectangular isotropic plate models: (a) plate model with CF strips; (b) plate model with SF strips.).

CF strips have been located before casting of concrete considering a cover of width about 15 mm. A net of steel bars with a diameter of 5 mm has been positioned at the extrados of the plate. The yield strength of steel bars was equal to $f_y \geq 380$ N/mm^2. The average concrete strength for plate model of Fig. 1(a) was about $f_c \cong 20$ N/mm^2 and the Young's modulus equal to $E_c \cong 20$ kNmm^{-2}. It was evaluated indirectly by the formula $E_c = 4500\sqrt{f_c}$, where f_c is the compressive strength.

The second plate model has been reinforced with strips of steel fibres (SF) embedded in concrete (Fig. 1(b)). Strips have been orthogonally located on a plane at 15 mm from surface with 15 strips each of width 50 mm. The average concrete strength for plate model of Fig. 1(b) was about $f_c \cong 30$ N/mm^2. The tensile strength was evaluated experimentally equal to $f_{ct} \cong 3$ N/mm^2.

In both plates the area of fibres was about 12 mm^2 for an interval of length of 200 mm. Figure 2 shows carbon and steel fibres used for strengthening the isotropic plates. Steel fibres were characterized by strand with five wires of area 0.096 mm^2 for each wire and about 2.27 mm^2/cm and Young's modulus equal to $E_s \cong 206$ kNmm^{-2}.

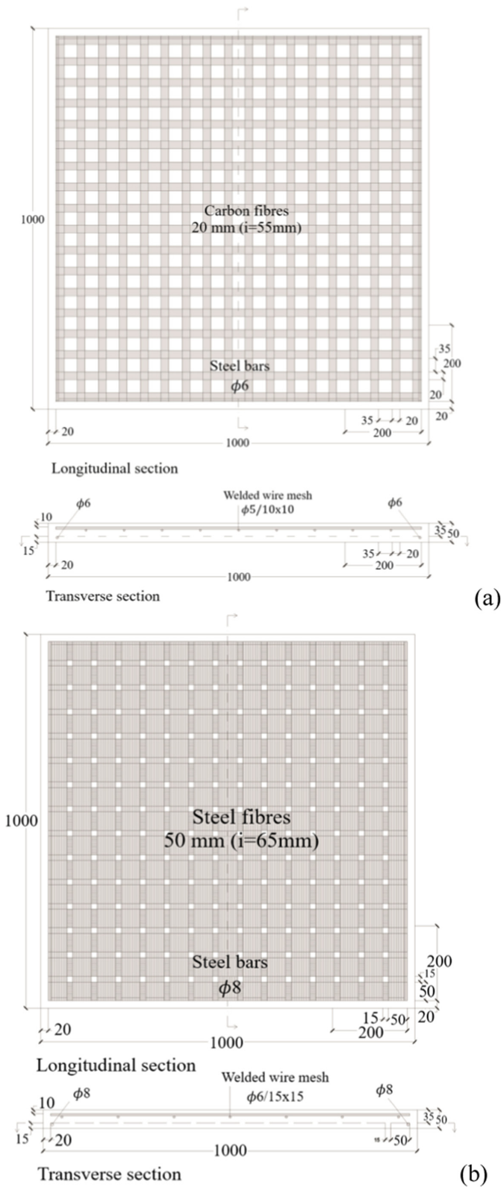

Fig. 1. Rectangular isotropic plate models: (a) plate model with CF strips; (b) plate model with SF strips.

Setup of loading tests for concrete plates is shown in Fig. 3. The plate was disposed in vertical with a contrast due to a steel frame and subjected to loading applied on a central surface by a steel plate connected with a hydraulic jack. The instruments used in the experimental tests were: one loading cell to measure transmitted load, P, on the central area of the plate of dimensions 300 mm·300 mm; five linear transducers (LVTDs) to measure deflections at five points on the bottom surface of the plate; four strain gauges located at the centre of the plate along both directions and on both concrete plate surfaces to measure strains.

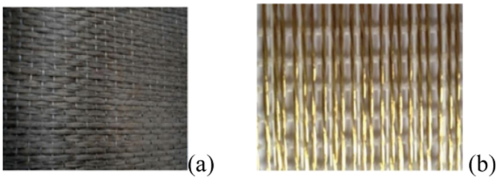

Fig. 2. (a) Carbon fibres; (b) steel fibres.

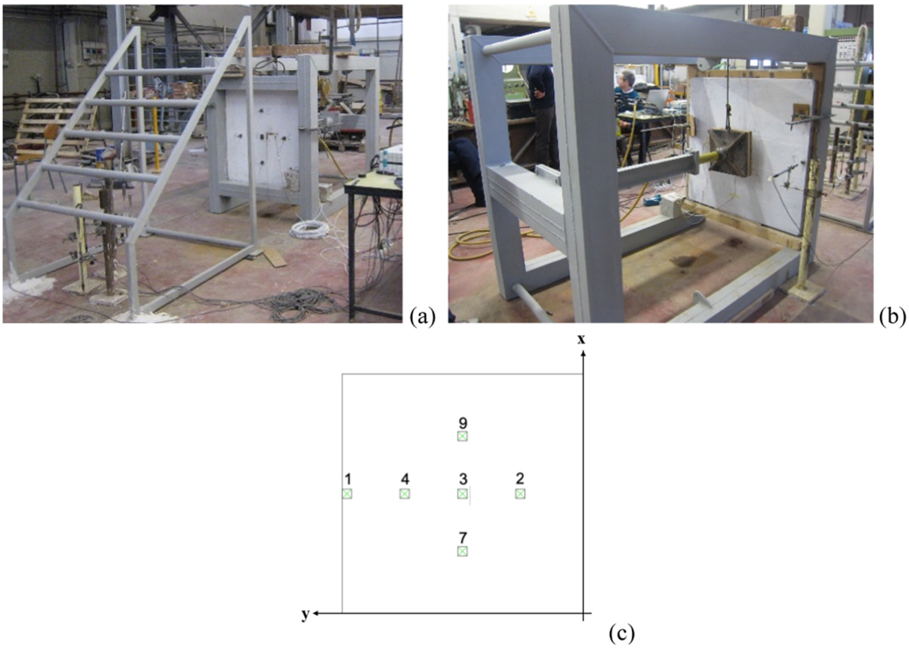

Fig. 3. Setup of tests for isotropic concrete plates: (a) view of intrados and (b) extrados side and (c) (c) points of measure for deflections.

2.2 Orthotropic Plate Model

One concrete orthotropic plate model reinforced with embedded CFRP Rods has been subjected to the same load distributed on a square surface of 300 mm·300 mm on the upper surface of the concrete plate [17].

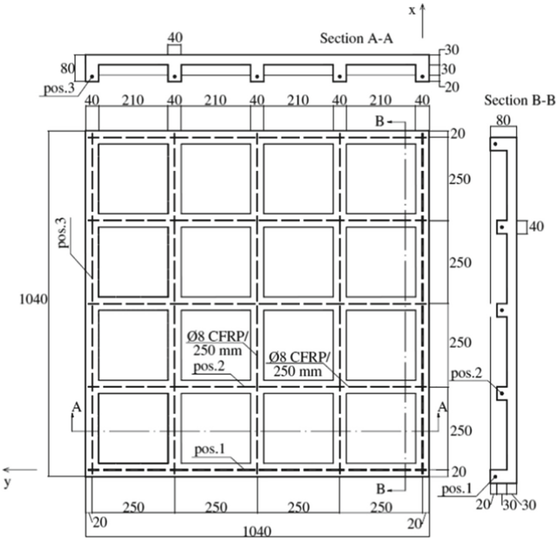

Fig. 4. Rectangular orthotropic plate model with CFRP rods.

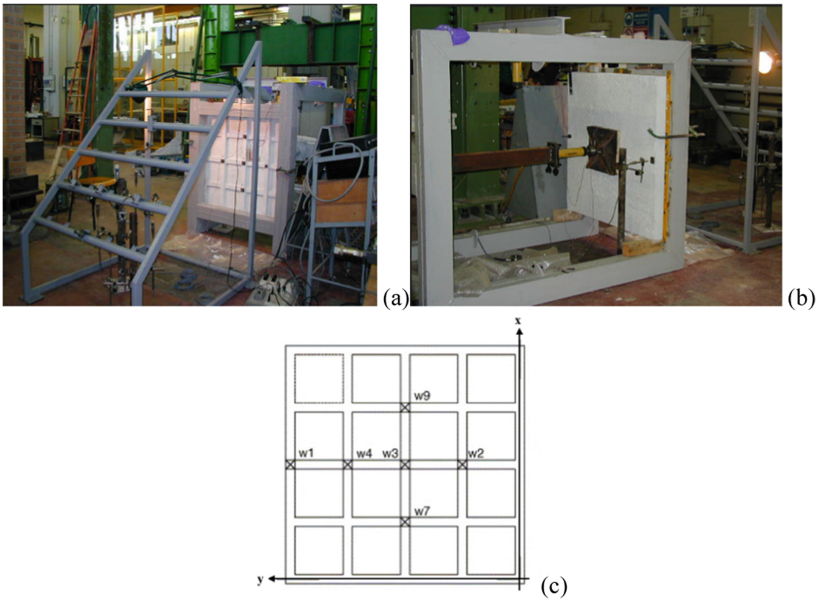

Fig. 5. Setup of tests for orthotropic plate model: (a) view of intrados and (b) extrados side and (c) points of measure for deflections.

This experimental plate model is characterized by two orders of concrete beams in the plane principal directions. The concrete plate measured 1.0 m·1.0 m in plan with a thickness of 30 mm. The dimensions of main ribs section were 40 mm·80 mm and

40 mm·60 mm for perpendicular ribs at constant interval of 250 mm (Fig. 4). The average concrete strength for plate model was about $f_c \cong 20$ N/mm^2. Smooth steel bars of diameter 5 mm were arranged in the concrete slab as steel net with 100 mm intervals. The model has been strengthened with CFRP rods of diameter 8 mm in every ribs.

The load was transmitted by a hydraulic controlled jack (Fig. 5). The deflections were measured by six LVTDs: five of them were positioned in the principal concrete ribs and one was positioned in the concrete slab on the upper surface; four strain gauges were located both at the intrados and at the extrados of the concrete slab.

3 Experimental Results

The three concrete plate models were subjected to bending test under an increasing vertical load until failure. The flexural behaviour of the three plates is shown in terms of cracking phases and deflection values.

Isotropic Plates

The isotropic thin plates were subjected under increasing load up to failure. For the plate model reinforced with CF embedded in concrete, first cracks were detected at about P = 6 kN during the test, while failure was recorded for a load equal to P = 26 kN. This failure was associated with an increasing cracking in the bottom surface of the plate (Fig. 6).

Fig. 6. Cracking at failure of plate with carbon fibres.

Table 1 shows some deflection values of the five control points (Fig. 3(c)) at bottom surface as the vertical load P increases during the bending test.

Table 1. Deflection values at bottom surface of plate with carbon fibres.

P (kN)	w_2 – A (mm)	w_3 – B(mm)	w_4 – C (mm)	w_7 – D (mm)	w_9 – E (mm)
0.00	0.000	0.000	0.000	0.000	0.000
6.00	0.209	0.462	0.224	0.415	0.140
10.00	1.573	2.817	1.873	2.842	1.185
16.00	8.877	15.177	10.186	11.936	9.174
18.00	10.380	17.692	11.867	13.667	10.795
20.00	12.968	21.843	14.634	16.597	13.525
24.00	16.774	27.846	18.733	20.783	17.627
26.00	19.764	32.436	22.033	23.955	20.952

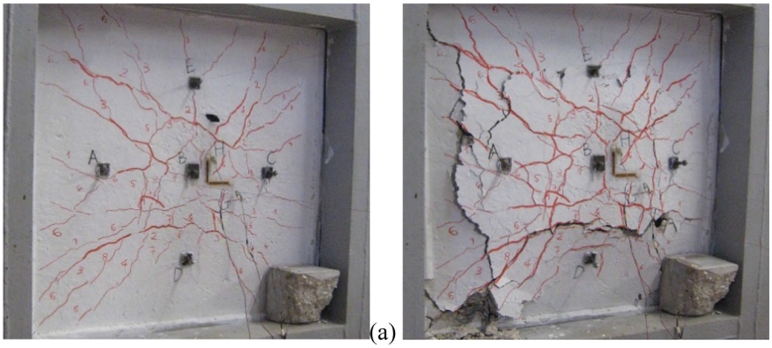

(a) (b)

Fig. 7. Cracking phases of plate with steel fibres: (a) at P = 26 kN and (b) at punching failure.

The plate reinforced with steel fibres showed first cracks at about P = 11 kN during the test and a diffused cracking phenomenon on the bottom concrete surface for load equal to P = 26 kN (Fig. 7(a)). Failure load was equal to about P ≅ 64 kN with punching (Fig. 7(b)). In Table 2 some deflections values of the five control points (Fig. 3(c)) at the bottom surface are shown.

Orthotropic Plate

For the orthotropic plate model with embedded CFRP rods, the bending test was developed by two cycles of loading: at first, the vertical load was applied until the formation of the first cracks, which were recorded for a load value approximately equal to P ≅ 10.7 kN; then, at the second cycle, the vertical load was monotonically increased until the failure of experimental model at the value of load equal to P ≅ 30 kN. At this failure load, cracks totally interested the intrados surface of the concrete plate (Fig. 8). Table 3 shows some deflection values, of the six control points (Fig. 5(c)), recorded for the two phases of loading.

Table 2. Deflection values at bottom surface of plate with steel fibres.

P (kN)	w_2 – A (mm)	w_3 – B (mm)	w_4 – C (mm)	w_7 – D (mm)	w_9 – E (mm)
0.00	0.000	0.000	0.000	0.000	0.000
9.006	0.287	0.509	0.387	0.315	0.484
10.006	0.565	0.934	0.659	0.528	0.718
12.012	0.571	1.353	0.909	0.709	0.971
18.060	3.759	6.384	3.828	3.959	4.031
20.026	4.553	7.631	4.559	4.775	4.656
26.012	8.100	12.881	7.834	8.409	7.868
40.038	12.671	19.943	11.550	12.928	11.440
42.197	13.134	20.753	11.937	13.659	11.853
60.017	18.059	28.353	15.640	18.606	15.618
63.892	20.528	33.631	17.178	21.934	17.581

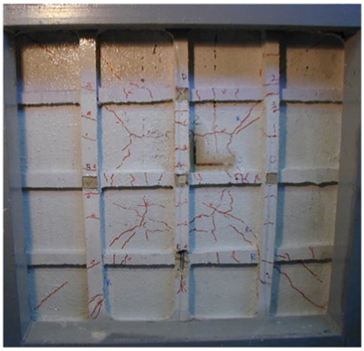

Fig. 8. Cracking at failure of orthotropic plate.

4 Discussion

Below are the graphs deduced from the experimental tests related to the three models of concrete plates. Figure 9 shows a comparison between the experimental curves Load, P, versus Deflection, w, of the two models of isotropic concrete plates. Diagrams present the deflection values recorded in three points of the plate where the transducers were placed, points A, C and D respectively. In the experimental curves related to the plate reinforced with CF strips, it is possible to identify a bilinear trend, with two decreases in slope. The first stage describes a linear elastic behaviour up to the value of load corresponding to the cracking of tensile concrete; the second is the inelastic phase, with loss of stiffness and increase of displacement up to failure load.

The experimental diagrams of the plate reinforced with SF strips show a trilinear trend, with a third phase characterized by the resistance of the fibres that determine an

Table 3. Deflection values at bottom surface of orthotropic plate with CFRP rods.

P (kN)	w_3 – A (mm)	w_2 – B (mm)	w_4 – C (mm)	w_9 – D (mm)	w_7 – E (mm)	w_1 (mm)
0.00	0.000	0.000	0.000	0.000	0.000	0.000
1.00	0.037	0.000	0.022	0.053	0.053	–0.003
2.00	0.162	0.034	0.103	0.147	0.162	−0.008
4.00	0.693	0.403	0.566	0.431	0.637	−0.001
7.00	1.743	1.156	1.400	1.087	1.565	0.133
10.70	3.184	2.109	2.422	2.068	2.686	0.454
1.00	1.487	1.153	1.268	0.934	1.384	0.411
2.00	1.671	1.222	1.368	1.072	1.544	0.392
4.00	2.121	1.484	1.650	1.353	1.944	0.414
7.00	2.787	1.881	2.128	1.797	2.468	0.527
13.00	5.006	3.395	3.620	3.262	4.194	0.819
20.00	9.403	6.366	6.556	6.100	7.406	1.026
25.00	12.315	8.496	8.537	7.947	9.844	1.163
30.00	15.256	10.547	10.500	9.810	11.850	1.343

increase in stiffness up to the failure of punching. The plate reinforced with SF strips exhibited widespread cracking for a load value equal to P = 26 kN, corresponding to the failure load for the plate reinforced with CF strips. However, from the comparison between the experimental graphs of Fig. 9, at the load P = 26 kN, the plate reinforced with SF strips showed deflections about 2.5 times smaller. In Fig. 10 the experimental diagram, Load, P, versus Deflection, w, at the centre of the orthotropic model reinforced with CFRP bars is shown.

From the analysis of the flexural behaviour of the beam grid model in terms of deflections until failure, it can be deduced that three phases describe the response under load of the reinforced plate model: after an un-cracked first phase, up to $P < 4$ kN, the second phase is characterized by an elastic behaviour after cracking of concrete, for load values approximately between 4 and 11 kN; the deflection values increase in the third inelastic phase, for a load value $P > 11$ kN.

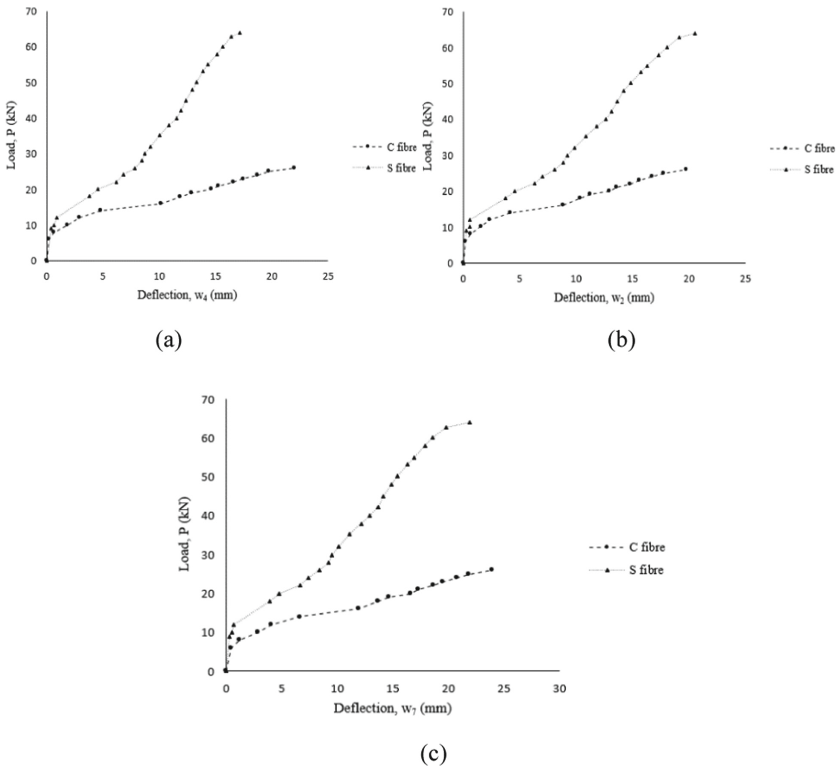

Fig. 9. Comparison of exp. Diagrams load, P, vs. deflection values for isotropic plates, recorded at the points: (a) w2 – A; (b) w4 – C; (c) w7 – D.

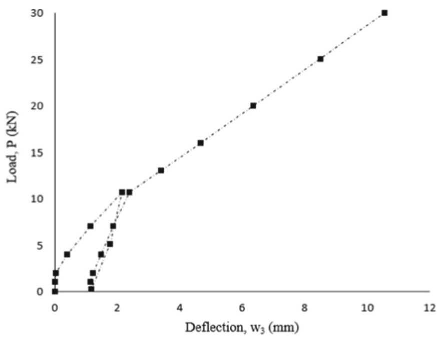

Fig. 10. Exp. Diagram load, P, vs. deflection for orthotropic plate, recorded at the point W3-A.

5 Conclusions

This paper deals about the analysis of the behaviour of concrete rectangular plates without steel bars reinforcing in tension.

Bending tests were carried out on three concrete plate models: two isotropic and one orthotropic rectangular concrete plate reinforced, respectively, with carbon fibre polymer (CFRP) rods and carbon/steel fibre (C/SF) strips embedded in concrete in the tensile side. From the analysis of the experimental results, the following conclusions can be drawn:

– The use of dry fibres as a net in the tensile concrete zone is a valid method for reinforcing concrete thin plates, in place of steel bars.
– The bond mechanisms have a great influence on the response.
– The bending behaviour of the concrete plate reinforced with steel fibres shows smaller deflections and greater strength than the carbon strips.
– The behaviour of the orthotropic plate model with CFRP rods is adequate to although width of cracks mostly influences the response under loading.

Acknowledgments. The Authors wish to thank all the technicians and students who worked to carry out the experimental tests. The experimental research was developed through founds provided by Polytechnic University of Marche, Italy.

References

1. Capozucca, R., Magagnini, E.: Vibration of RC beams with NSM CFRP with unbonded/notched circular rod damage. Compos. Struct. **144**, 108–130 (2016)
2. Bendada, A., Boutchicha, D., Khatir, S., Magagnini, E., Capozucca, R., Abdel, W.M.: Mechanical characterization of an epoxy panel reinforced by date palm petiole particle. Steel Compos. Struct. **35**(5), 627–634 (2020)
3. Capozucca, R., Magagnini, E., Vecchietti, M.V.: Experimental static and dynamic response of RC beams damaged and strengthened with NSM GFRP rod. Compos. Struct. **241**, 112100 (2020)
4. Capozucca, R., Magagnini, E.: RC beam models damaged and strengthened with GFRP strips under bending loading and free vibration. Compos. Struct. **253**, 112730 (2020)
5. Capozucca, R., Magagnini, E., Bettucci, E.: Delamination buckling of GFRP-strips in strengthened RC beams. Compos. Struct. **300**, 116183 (2022)
6. Capozucca, R.: Assessment of CFRP Strengthened RC beams through dynamic tests. Comp. Part. B: Eng. **46**, 69–80 (2013)
7. Nabil, F.G., Abdel-Sayed, G., Wahba, J., Sakla, S.: Mathematical solution for carbon fiber-reinforced polymer prestressed concrete skew bridges. ACI Struct. J. **96**(6), 981–987 (1999)
8. Michaluk, C.G., Rizkalla, S.H., Tadros, G., Benmokrane, B.: Flexural behavior of one-way concrete slabs reinforced by fiber reinforced plastic reinforcements. ACI Struct. J. **95**(3), 353–363 (1998)
9. Zhang, B., Masmoudi, R., Benmokrane, B.: Behaviour of one-way concrete slabs reinforced with CFRP grid reinforcements. Construct. Build Mater. **18**(8), 625–635 (2004)
10. Shill, S.K., Garcez, E.O., Al-Ameri, R., Subhani, M.: Performance of two-way concrete slabs reinforced with basalt and carbon FRP rebars. J. Compos. Sci. **6**, 74 (2022)
11. Aljazaeri, Z., Alghazali, H.H., Myers, J.J.: Effectiveness of using carbon fiber grid systems in reinforced two-way concrete slab system. ACI Struct. J. **117**, 81–89 (2020)

12. El-Gamal, S., El-Salakawy, E., Benmokrane, B.: Behavior of concrete bridge deck slabs reinforced with fiber-reinforced polymer bars under concentrated loads. ACI Struct. J. **102**, 727 (2005)
13. Yost, J.R., Goodspeed, C.H., Schmeckpeper, E.R.: Flexural performance of concrete beams reinforced with FRP grids. J. Compos. Constr. **5**, 18–25 (2001)
14. Borri, A., Castori, G., Grazini, A., Giannantoni, A.: Composites SRP/SRG: characteristics, testing and applications. Build. Masonry **117**, 52–57 (2006)
15. Mahroug, M., Ashour, A., Lam, D.: Tests of continuous concrete slabs reinforced with carbon fibre reinforced polymer bars. Compos. Part B Eng. **66**, 348–357 (2014)
16. Banthia, N., Al-Asaly, M., Ma, S.: Behavior of concrete slabs reinforced with fiber-reinforced plastic grid. J. Mater. Civ. Eng. **7**, 252–257 (1995)
17. Capozucca, R.: Analysis of the experimental flexural behaviour of a concrete beam grid reinforced with C-FRP bars. Comp. Struct. **79**(4), 517–526 (2007)
18. Ouladbrahim, A., Belaidi, I., Khatir, S., Magagnini, E., Capozucca, R., Wahhab, M.A.: Prediction of gurson damage model parameters coupled with hardening law identification of Steel X70 pipeline using neural network. Met. Mater. Int. **28**, 370–384 (2022)
19. Khatir, S., Tiachacht, S., Le Thanh, C., Ghandourah, E., Mirjalili, S., Wahab, M.A.: An improved artificial neural network using arithmetic optimization algorithm for damage assessment in FGM composite plates. Compos. Struct. **273**, 114287 (2021)
20. Razavi, S.V., Ayazi, M.H., Mohammadi, P.: Artificial neural network for structural behavior prediction of RC one-way slab strengthened by CFRP. Sci. Res. Essays **6**(23), 5609–5627 (2011)
21. Capozucca, R., Bossoletti, S., Gabrielloni, M.: Response of concrete plates reinforced with carbon-basalt-steel fibres under loading. In: Proceedings Fibre Concrete 2013, 12–13 September, 2013, Prague, Czech Republic (2013)